Observation of Reentrant 2D to 3D Morphology Transition in Highly Strained Epitaxy: InAs on GaAs

R. Heitz, T. R. Ramachandran, A. Kalburge, Q. Xie, I. Mukhametzhanov, P. Chen, and A. Madhukar
Photonic Materials and Devices Laboratory, Departments of Materials Science and Physics, University of Southern California, Los Angeles, California 90089-0241
(Received 19 September 1996)

The two-dimensional (2D) to three-dimensional (3D) transition in highly strained growth of InAs of GaAs(001) is investigated using *in situ* scanning tunneling microscopy and photoluminescence spectroscopy. Remarkably, InAs structural features up to five monolayers (ML) high appear at ~1.25 ML, disappear, and reappear prior to the onset of well-developed 3D islands at 1.57 ML, thus manifesting a hitherto unrecognized reentrant behavior in the formation of 3D islands. The results provide new insights into the long-standing problem of the kinetic aspects of 2D to 3D morphology change not embodied in the widely encountered Stranski-Krastanow growth mode. [S0031-9007(97)03235-3]

PACS numbers: 68.35.Bs, 61.16.Ch, 78.66.Fd

The surface morphology of overlayers having a high lattice mismatch with substrates has, for a wide variety of combinations, been found to change from an initially two-dimensional (2D) to a three-dimensional (3D) island-like nature beyond a (growth condition dependent) critical amount of material deposition (film thickness) [1]. Such a growth mode is referred to as the Stranski-Krastanow growth mode [2]. For nearly five decades it was assumed that the change from the planar 2D to 3D island morphology is accompanied by the formation of defects (such as dislocations). Indeed, a school of thought attributed the initiation of 3D islands itself to the appearance of dislocations [3]. However, the reports some six years ago that, in the semiconductor systems InGaAs on GaAs [4] and Ge on Si [5], coherent (i.e., defect-free) 3D islands can form have led to intensive efforts towards a better atomistic and kinetic understanding of the actual pathway from 2D to 3D morphology [6–12]. On the pragmatic side, the coherent nature of the 3D islands has, in the past three years, caused explosive growth in the examination of their optical behavior as quantum boxes [dubbed quantum dots (QDs)] [10,13–17] and of their potential for QD-based injection lasers [18,19]. Indeed, understanding the atomistic mechanism of strain-induced evolution of the 3D islands is fundamental for exploiting concepts of self-assembly and/or self-ordering [20] in order to realize the desired electronic and optical properties of the QDs. This demands careful and systematic atomic level structural [such as provided by a scanning tunneling microscope (STM)] and optical studies carried out on comparable samples. In this Letter we report on the results of such a study undertaken for the InAs/GaAs(001) system (lattice mismatch ~7%) for InAs depositions from submonolayer to just above 2 monolayers (ML). The STM results reveal, and the optical results independently confirm, a highly unexpected reentrant nature of the formation of 3D-like features with increasing InAs deposition, in which 3D-like features appear well in advance of the stage of 3D island formation, disappear, and then reappear just prior to the onset of coherent 3D island formation. The observations thus provide clear evidence that the change from 2D to 3D morphology in highly strained growth is more subtle and complex than the spontaneous change from 2D to 3D morphology embodied in current descriptions of Stranski-Krastanow growth mode [12].

Samples for STM investigation were grown via molecular beam epitaxy on n^+-GaAs(001) ($\pm 0.1°$) substrates using the same growth conditions as in Ref. [11]. InAs was deposited at 500 °C on a 500 nm GaAs buffer showing clear $c(4 \times 4)$ reconstruction at a growth rate of 0.22 ML s^{-1} and an As_4 partial pressure of 6×10^{-6} Torr. The InAs deposition amount, given with respect to the GaAs surface density, was reproducible to within 0.022 ML. Weak spots superposed on faint streaks appeared at 1.57 ML coverage (denoted Θ_C) in the reflection high energy electron diffraction pattern, signifying the onset of 3D island formation. The samples were cooled down immediately after InAs deposition to keep postgrowth surface evolution to a minimum. Samples for photoluminescence (PL) and PL excitation (PLE) investigation were grown on semi-insulating substrates in exactly the same way, with the GaAs cap layer grown at 400 °C by migration enhanced epitaxy [14].

Figure 1 shows typical STM images for InAs deliveries from 0.87 to 1.61 ML. The images reveal 1 ML high steps (labeled *S*) corresponding to 200–400 nm wide terraces, consistent with a substrate tilt less than 0.1°, and a high density ($>10^{11}$ cm^{-2}) of up to a few nm wide and 1 ML high clusters referred to here as small 2D clusters (labeled *A*, lateral size <20 nm). The first InAs layer [referred to as the wetting layer (WL) hereafter] is found to be incomplete up to 1.35 ML InAs delivery, showing 1 ML deep holes (labeled *H*). At 0.87 ML [panel (a)] the holes cover about 20% of the surface consistent with the observed steps corresponding basically to those of the GaAs substrate. Further InAs deposition [1.15 ML, panel

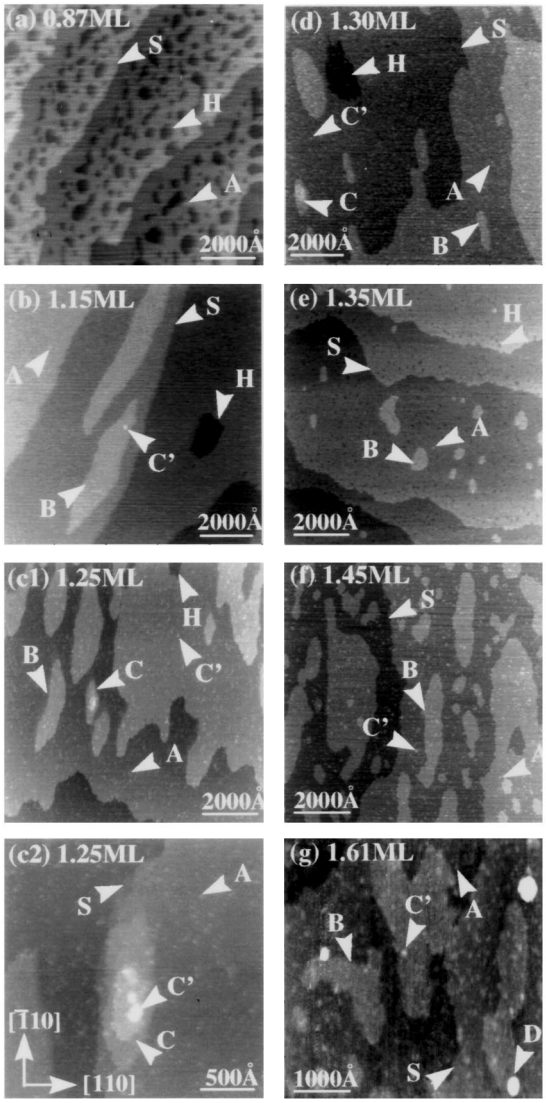

FIG. 1. STM images showing the evolution of InAs on GaAs(001) for depositions of (a) 0.87, (b) 1.15, (c1, c2) 1.25, (d) 1.30, (e) 1.35, (f) 1.45, and (g) 1.61 ML. The labels in the figure denote small 2D clusters (A), large 2D clusters (B), small Q3D clusters (C'), large Q3D clusters (C), 3D islands (D), 1 ML high steps (S), and 1 ML deep holes (H).

(b)] leads to the formation of 1 ML high clusters with lateral sizes up to hundreds of nm, referred to here as large 2D clusters (labeled B, lateral size $\geq$50 nm), on top of the still incomplete WL. These large 2D clusters are elongated in the $[\bar{1}10]$ direction. Strikingly, at this deposition of 1.15 ML, the InAs surface starts to also show features that are 2–4 ML high (counted from the flat InAs surface) and up to 20 nm wide (labeled C'), which we will call *small* quasi-3D (Q3D) clusters. Although in the STM images the small Q3D clusters appear to be similar to small 2D clusters (A), cross-sectional profiles (not shown here) reveal that the former are $\geq$2 ML in height, whereas the latter are 1 ML high. At 1.25 and 1.30 ML InAs delivery [panels (c1) and (d)], in addition to the small Q3D clusters, clusters of similar height (2–4 ML) but lateral extension $\geq$50 nm are present (labeled C), which we will call *large* Q3D clusters. In addition, we observe features up to 5 ML high which have an extended base and a narrow top [panel (c2)]. In anticipation of the consequences of such structural characteristics for the optical results discussed later, we classify these features as a large Q3D cluster (C) topped by a small one (C') as marked in Fig. 1(c2). Remarkably, the Q3D clusters (small and large) *disappear* as the InAs delivery is increased to 1.35 ML [panel (e)], resulting again in a 2D-like surface. As the InAs deposition is further increased to 1.45 ML [panel (f)] only *small* Q3D clusters *reappear* at a 2 orders of magnitude higher density. This is well in advance of the emergence of the first 3D islands labeled D in panel (g), typically 7–14 ML high with a lateral size $<$25 nm, observed for $\Theta \geq \Theta_C$ ($\sim$1.57 ML). Between 1.57 and 1.74 ML depositions we find coexisting 2D clusters, small Q3D clusters, and 3D islands, as shown for 1.61 ML deposition [panel (g)].

The density evolution of the 2D clusters, Q3D clusters, and the 3D islands with increasing InAs deposition is summarized in Fig. 2. The densities are averaged from up to 100 μm^2 of investigated surface. The Q3D cluster density behavior unambigously demonstrates the previously undetected appearance, disappearance, and reappearance of 3D morphological features well in advance of the regime ($\Theta \geq \Theta_C$) of well-formed 3D islands identified in earlier studies [4,8–11].

The unanticipated presence and behavior of the Q3D clusters prompted us to undertake systematic PL and PLE studies of an equivalent set of capped samples. The

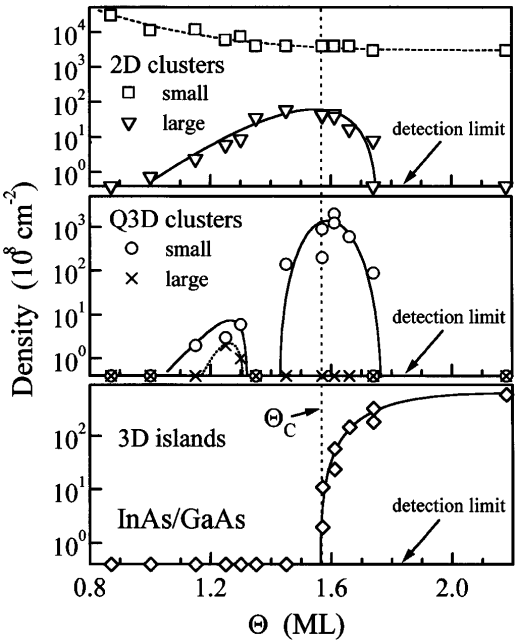

FIG. 2. Area density of 2D and Q3D clusters as well as 3D InAs islands on GaAs(001) as a function of InAs deposition. The densities are determined from up to 100 μm^2 of STM images.

structural knowledge of the deposition amount dependent InAs morphology established in the STM investigations allows, as shown below, a detailed and consistent interpretation of the optical spectra. Figure 3 shows the evolution of the PL spectra from 1.00 to 2.00 ML InAs deposition excited with an Ar^+ laser at a density of 5 $W\,cm^{-2}$. The narrow peak near 1.45 eV, which evolves with increasing InAs deposition and vanishes just beyond Θ_C, is attributed to recombination in the WL, and the almost Gaussian peak observed at 1.215 eV for the 2.00 ML sample is attributed to recombination in 3D island QDs [10,14–16]. A careful analysis of the PL spectra of the 1.15 and 1.25 ML samples reveals, for the first time, peaks at 1.322 and 1.274 eV, respectively, in addition to the WL emission. By contrast, no PL in the 1.20 to 1.35 eV region could be resolved for the 1.35 and 1.45 ML samples. And then, at 1.55 ML deposition (just below Θ_C), PL reappears in this spectral region and finally develops into 3D island PL, thus establishing a reentrant PL behavior paralleling that of the 3D structural features seen in the STM studies (Figs. 1 and 2).

The large 2D and large Q3D clusters have a lateral extension larger than the exciton Bohr diameter and therefore provide no, or only weak, lateral electronic confinement. Thus, these structural features constitute 2 ML or thicker InAs regions which behave like quantum wells whose fundamental transitions are expected to be below 1.4 eV [21]. Thus, we relate the low energy (1.322 and 1.274 eV) PL peaks in the 1.15 and 1.25 ML samples to the large 2D and large Q3D clusters acting as locally thicker wetting layer-like regions. This is further supported by PLE spectra for the above two samples excited with a Ti-sapphire laser, as shown in Fig. 4. The PLE efficiency for these emissions reaches a maximum at about 25 meV above the detection energy and then decreases gradually with increasing excitation energy, indicating a continuous density of states. We attribute the PLE maxima to intrinsic absorption in the large 2D and large Q3D clusters, whereas the PL is mediated by localized electronic states causing a 25 meV decrease in the PL energy. A comparison with the STM information on the morphology of the InAs layer suggests that *small* Q3D clusters (i.e., feature C' in Fig. 1) on top of large 2D and large Q3D clusters act as optically active QDs. The lateral size and height of the small Q3D clusters are consistent with a localization energy of 25 meV [21].

The observation of emission from the composite structure of small Q3D clusters on large 2D clusters also explains the disappearance of the PL in the 1.20 to 1.35 eV range for the 1.35 ML sample (see Fig. 3) having 4×10^9 cm^{-2} large 2D clusters but no small Q3D clusters, and indicating dominant nonradiative recombination in the large 2D clusters [22]. The consequently reduced lateral carrier diffusion in the large 2D clusters hampers diffusion-related optical excitation of the small Q3D clusters (if present) as is supported by the absence of a resonance due to the WL absorption in the PLE spectra of the 1.322 and 1.274 eV peaks in the 1.15 and 1.25 ML samples, respectively (Fig. 4, the arrows mark the position of the WL PL peak).

The structural and optical results above provide for the first time a detailed picture of the kinetically controlled evolution of the InAs surface. InAs is incorporated in higher layers even before the first InAs layer is

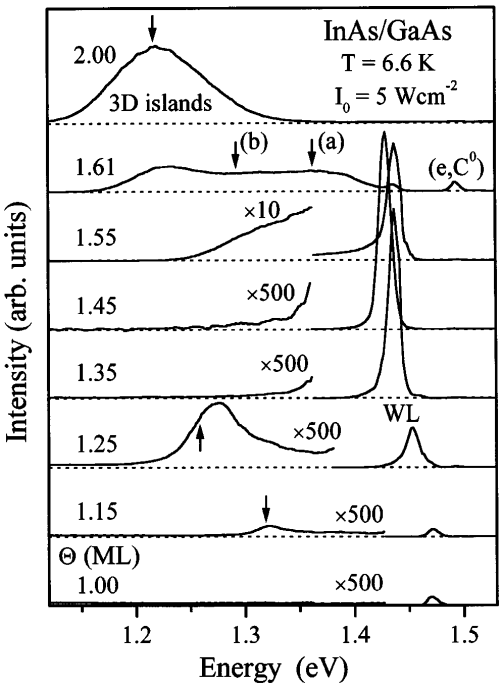

FIG. 3. PL spectra for InAs on GaAs(001) at various depositions Θ, excited at 514 nm with a density of 5 $W\,cm^{-2}$. The arrows mark the detection energies for the PLE specta shown in Fig. 4. The peak at 1.493 eV (1.61 ML sample) is attributed to carbon-related recombination in the GaAs barrier.

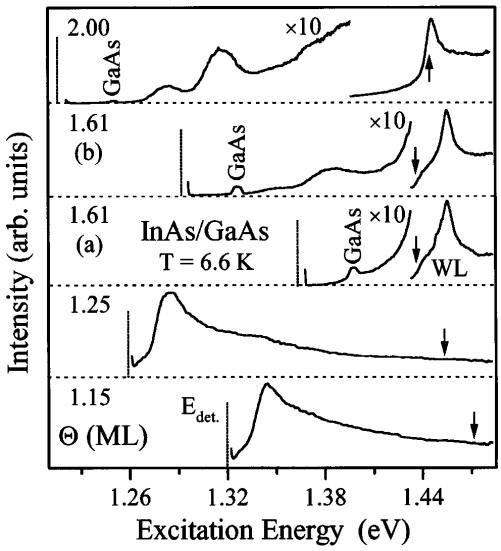

FIG. 4. PLE spectra for InAs on GaAs(001) with various depositions Θ below and above Θ_C. The arrows mark the energy position of the respective WL PL peak. The weak peaks marked "GaAs" in the PLE of the 1.61 and 2.00 ML samples result from GaAs Raman scattering.

completed. In addition to 2D clusters, Q3D clusters form for depositions as low as 1.15 ML due to the strain-driven surface kinetics near the cluster edges. On the one hand, the In migration length of 280 nm under the employed growth conditions [20] exceeds the separation and size of the large 2D clusters, making statistical initiation of new layers on top of them unlikely. On the other hand, the strain fields at the edges of 2D clusters lead to an asymmetry in interplanar In diffusion [6], making the formation of Q3D clusters possible. The disappearance of the Q3D features above 1.30 ML is thus likely related to the synergistic change in the surface strain fields when the first InAs ML nears completion.

The reappearance of the small Q3D clusters with a further increase in Θ (Fig. 2) leads to a low energy tail in the WL peak in PL (Fig. 3 for 1.55 ML). Indeed, the high density of small Q3D clusters (2×10^{11} cm^{-2} at 1.61 ML, corresponding to an average separation of 22 nm) indicates that they act as precursors of 3D islands. This is emphasized by the PLE spectra (Fig. 4) for the 1.61 ML sample [taken at detection energies marked (a) and (b) in Fig. 3], showing that the carrier localization gradually increases to that of the 3D islands (2.00 ML sample) with decreasing recombination energy. The small Q3D clusters start to grow into 3D islands, resulting in a decreasing vertical confinement. The low near-resonant PLE efficiency, followed by a series of excitation peaks, is characteristic of 3D island QDs [14,16], and the high excitation efficiency via the WL unambiguously locates the growing Q3D clusters as well as the 3D islands directly on top of the WL.

Finally, we comment on the emission observed between 1.43 and 1.47 eV. In optical studies [10,14], this regime of emission has been identified with the notion of a WL. The STM images show most of the sample surface to be covered by 1 ML thick InAs regions, which leads us to attribute this emission, which dominates the PL spectra as long as no 3D islands are present, to 1 ML thick InAs regions (the WL) that act as quantum wells. The WL emission shifts towards lower energies with increasing deposition below Θ_C (Fig. 3) and shows superlinear dependence of the intensity on InAs deposition from 1.15 to 1.35 ML. This is likely indicative of the synergistic changes in the strain relaxation and the degree of the first ML completion as the 3D features appear and disappear in this regime, but further studies are needed to sort out what is probably a very complex behavior. For depositions $\Theta \geq 1.74$ ML the WL appears at (1.448 ± 0.003) eV with a Stokes shift of $\sim$4 meV (Fig. 4), indicating the high quality of the WL in the 3D growth regime.

In conclusion, we have presented direct structural and supporting optical evidence for a reentrant behavior in the 2D to 3D morphology change during growth of highly strained InAs on GaAs. The key role in the formation of 3D features is played by Q3D clusters which form for deliveries as low as 1.15 ML, vanish at 1.35 ML, reestablishing a 2D surface, and reappear just prior to Θ_C ($\sim$1.57 ML), acting as precursors to 3D islands. Our results reveal for the first time that a clearer and more accurate description of the change from 2D to 3D morphology requires the development of a theoretical framework that explicitly accounts for the synergistic kinetics of strained growth as a function of increasing deposition, and thus goes beyond the spontaneous change embodied in the thermodynamic equilibrium-based current descriptions [12] of the Stranski-Krastanow growth mode. Finally, the small Q3D clusters of less than 20 nm lateral extension and 2–4 ML height on 2 ML and thicker InAs regions lead to PL in the 1.20 to 1.35 eV range, giving optical access to the nonequilibrium morphology of the WL.

This work was supported by the U.S. AFOSR, ARO, and ONR.

[1] See, for example, *Strained-Layer Superlattices: Physics*, Semiconductors and Semimetals Vol. 32, edited by T. P. Pearsall (Academic Press, Boston, 1990); *Strained-Layer Superlattices: Materials Science and Technology*, Semiconductors and Semimetals Vol. 33 (Academic Press, Boston, 1991).
[2] I. N. Stranski and L. Krastanow, Sitzungsber. Wien. Akad. Wiss. Math.-Nat. Kl. IIb **146**, 797 (1938).
[3] G. L. Price, Phys. Rev. Lett. **66**, 469 (1991), and references therein.
[4] S. Guha, A. Madhukar, and K. C. Rajkumar, Appl. Phys. Lett. **57**, 2110 (1990).
[5] D. J. Eaglesham and M. Cerullo, Phys. Rev. Lett. **64**, 1943 (1990).
[6] S. V. Ghaisas and A. Madhukar, J. Vac. Sci. Technol. B **7**, 264 (1989).
[7] Y.-W. Mo *et al.*, Phys. Rev. Lett. **65**, 1020 (1990).
[8] C. W. Snyder *et al.*, Phys. Rev. Lett. **66**, 3032 (1991).
[9] D. Leonard, K. Pond, and P. M. Petroff, Phys. Rev. B **50**, 11 687 (1994).
[10] J. M. Gerard *et al.*, J. Cryst. Growth **150**, 351 (1995).
[11] N. P. Kobayashi *et al.*, Appl. Phys. Lett. **68**, 3299 (1996); T. R. Ramachandran *et al.*, Appl. Phys. Lett. **70**, 640 (1997).
[12] C. Priester and M. Lannoo, Phys. Rev. Lett. **75**, 93 (1995).
[13] S. Fafard *et al.*, Appl. Phys. Lett. **65**, 1388 (1994).
[14] Q. Xie *et al.*, J. Cryst. Growth **150**, 357 (1995).
[15] M. Grundmann *et al.*, Phys. Rev. Lett. **74**, 4043 (1995).
[16] R. Heitz *et al.*, Appl. Phys. Lett. **68**, 361 (1996).
[17] A. Polimeni *et al.*, Phys. Rev. B **53**, R4213 (1996).
[18] D. Bimberg *et al.*, Jpn. J. Appl. Phys. **35**, 1311 (1996).
[19] Q. Xie *et al.*, IEEE Photon. Technol. Lett. **8**, 965 (1996).
[20] Q. Xie *et al.*, Phys. Rev. Lett. **75**, 2542 (1995).
[21] J.-Y. Marzin and G. Bastard, Solid State Commun. **92**, 437 (1994).
[22] The 1.45 ML sample shows no PL in the 1.20 to 1.35 eV region, though STM reveals small Q3D clusters [Fig. 1(f)]. Given the steep dependence of the small Q3D cluster density on Θ (Fig. 2), we attribute their absence in the capped sample to the uncertainty in Θ.